Neoplasma 2019; 66(6): 908–917

doi:10.4149/neo_2018_181205N923

miR-30a-5p modulates traits of cutaneous squamous cell carcinoma (cSCC) via forkhead box protein G1 (FOXG1)

J. SHAO[1,#], J. LIANG[1,#], S. ZHONG[2,*]

[1]*Department of Dermatology, Yantai Yuhuangding Hospital, Yantai, China;* [2]*Department of Dermatology, Yantai Yeda Hospital, Yantai, China*

**Correspondence: shanshanz_zhongss@163.com*
[#]Contributed equally to this work.

Received December 5, 2018 / Accepted April 29, 2019

miRNA has shown its potential in the regulation of squamous cell carcinoma (SCC). However, the mechanism of such an effect was not quite clear. Therefore, we aimed to investigate whether miR-30a-5p participated in the regulation of cutaneous SCC (cSCC) and the possible mechanism involved. 5-Ethynyl-2'-deoxyuridine (EdU) and cell cycle were measured using flow cytometry. The formation of cell colony was tested by colony formation assay. The capacities of migration and invasion were tested by wound healing assay and Transwell invasion assay, respectively. The target of miR-30a-5p was predicted by bioinformatics and identified by luciferase assay. Western blot was used for the determination of proteins and qPCR was for mRNA levels. miR-30a-5p expression was lowered in SCL-1 and A431 cells, and its upregulation suppressed EdU positive cells, colony numbers, migration, invasion and Bcl-2 expression, and elevated Bcl-2-associated X protein (Bax) and cleaved Caspase-3 expressions, arresting cell cycle in G1 phase. Moreover, forkhead box protein G1 (FOXG1) was proved to be the target of miR-30a-5p, and FOXG1 overexpression partially offsets the decreased colony numbers, migration and invasion rates due to miR-30a-5p overexpression in SCL-1 and A431 cells. miR-30a-5p showed a regulatory role on the expression of FOXG1 and further modulated the progressing of cSCC cells, which could be a novel pathway intervening the development of cSCC.

Key words: miR-30a-5p, cSCC, FOXG1, traits of cancer

Cutaneous squamous cell carcinoma (cSCC) is a malignant tumor originating from the epidermal or accessory keratinocytes and the leading cause of death from non-melanoma skin tumors [1–3]. Ultraviolet radiation is the main risk factor of cSCC, and other factors such as immunosuppression, human papillomaviruses (HPV) infection, chemical carcinogen contact etc. are contributed to the occurrence of cSCC as well [4–8]. Surgery has become a routine mean of removing skin tumors, such as Mohs surgery [9]. However, Mohs has a long operation time and high economic cost [9]. It is only suitable for a single focal, continuous growth of malignant tumors of the skin [9, 10]. Thus, it is of little significance for tumors with high metastatic or jumping growth properties [9, 11].

miRNAs are non-coding RNAs containing proximately 22 nucleotides and participate in the posttranscriptional regulation of target gene [12, 13]. miRNAs are proved to be critical in a plenty of biological activities and diseases, including tumorigenesis [12, 15]. Among all types of miRNAs, the regulatory role of miR-30a in squamous cell carcinoma has emerged. For instance, miR-30a-3p or 5p downregulation promoted the proliferation of esophageal squamous cell carcinoma cells [15]. Wang et al. also discovered that the invasion and metastasis of human head and neck squamous cell carcinoma were promoted by tumor growth factor (TGF)-β-induced signal transducer and activator of transcription 3 (STAT 3) overexpression via the interaction of metastasis associated lung adenocarcinoma transcript 1 (MALAT1) and miR-30a [16].

Nevertheless, no researches were found to identify the role of miR-30a in cSCC. Therefore, we aimed to investigate whether miR-30a-5p, one of the mature forms of miR-30a [17], was involved in the progressing of cSCC and its underlying mechanism. The disclosure of the role of miR-30a-5p in the regulation of cSCC would be benefit for the exploration of the molecular mechanism network of cSCC and the development of targeted agents.

Materials and methods

Cell culture, plasmid and transfection. HaCaT, SCL-1, A431 cell lines were provided by Shanghai Institute of Biochemistry and Cell Biology, Chinese Academy of Sciences

(CAS). All three cell lines were grown in RPMI-1640 medium containing 10% fetal bovine serum (FBS, Thermo Fisher, Waltham, USA), 50 U/ml penicillin and 50 µg/ml streptomycin (15070063, Thermo Fisher, Waltham, USA). Cells were grown in a humidified incubator filled with 5 % CO_2 at 37 °C and passaged 2–3 times per week. The miR-30a-5p mimic plasmid (miR-30a-5p mimic: 5'-UGUAAACAUCCUCGACUGGAAG-3'), forkhead box protein G1 (FOXG1) overexpression plasmid, FOXG1 overexpression negative control (NC) plasmid and the miRNA control plasmid were prepared by Shanghai Genepharma Company. pcDNA 3.1 was set as the vector of the building of plasmids. Cells were transfected with 100 nM RNA oligonucleotides or 1 µg plasmid DNA using Lipofectamine™ 2000 (Invitrogen, Waltham, USA).

Group. SCL-1, A431 cells were grouped according to the purpose of the present study.

- Group I: for the exploration of the effect of the overexpressed miR-30a-5p in SCL-1, A431 cell lines, cells were grouped as blank, miControl, miR-30a-5p mimic groups, which were treated with medium alone, miRNA control plasmid and miR-30a-5p mimic plasmid, respectively.
- Group II: for the confirmation of FOXG1 transfection efficiency, cells were grouped as blank, NC and FOXG1 groups, which were treated with medium only, FOXG1 overexpression negative control plasmid and FOXG1 overexpression plasmid, respectively.
- Group III: for the confirmation of FOXG1 transfection efficiency, cells were grouped as blank, miR-30a-5p mimic, NC, FOXG1, miR-30a-5p mimic + NC and miR-30a-5p mimic + FOXG1 groups, which were treated with medium alone, miR-30a-5p mimic plasmid, FOXG1 overexpression negative control plasmid, FOXG1 overexpression plasmid, miR-30a-5p mimic plasmid with FOXG1 overexpression negative control plasmid and miR-30a-5p mimic plasmid with FOXG1 overexpression plasmid, respectively.

EdU measurement by flow cytometry. After 72 h culturing, cells were diluted to 1×10^6 cells/ml in medium and tested by EdU Proliferation Assay Kit (ab219801, Abcam, San Francisco, USA). One ml of cells was transferred into flow test tubes and then added with 1 ml 1xEdU solution at 15 µM. Cells were collected by centrifugation at 300 xg for 5 min at 4 °C after the incubation of cells with EdU for 2 h. Cells were further fixed by 4% formaldehyde and permeabilized by Permeabilization buffer. The EdU was detected and analyzed on a flow cytometer at Ex/Em = 491/520 nm after the cells were treated with Reaction mix.

Cell cycle assessment by flow cytometry. After 72 h culturing, cells were diluted to 1×10^6 cells/ml in medium and the cell cycle was measured by Vybrant™ DyeCycle™ Violet Stain regent (Thermo Fisher, Waltham, USA). Briefly, according to the protocol provided by manufacturer, cell suspension was transferred to flow test tubes with the complete medium. Cells were treated with 1 µl Vybrant DyeCycle™ Violet stain diluted to 5 µM and then incubated for 30 min at 37 °C away from light. The 405 nm excitation and 440 nm emission of cells were then detected on a flow cytometer.

Colony formation assay. Followed by the transfection of miR-30a-5p or FOXG1 overexpression plasmid into the cells, 5×10^3 cells were seeded on a 6-well plate in 1 ml medium. Medium was changed every 3 days. 10 days (for Group I) or 48 h (for Group III) later, cell colonies were fixed with methanol and further stained with 0.5% crystal violet for 20 min. Colonies were scored under the microscope (Olympus IX71, Tokyo, Japan).

Wound healing assay. After trypsinization, cells were collected and seeded in a 6-well plates at density of 1×10^6 per well, and cultured until 90% confluence in medium. Monolayers of cells were scratched from up to down by a 200 µl pipette tip. Monolayers were then washed with PBS to remove cellular debris and further cultured for 24 h. Images of monolayers were captured under the inverted microscope (Olympus IX71, Tokyo, Japan) following wounding (0 and 48 h). The gaps between the leading edges on both sides were assessed using ImageJ software.

Transwell invasion assay. 3×10^4 cells in medium without serum were collected and transferred to the upper chamber of Transwell apparatus (8 µm, BD Biosciences, CA, USA) with a Matrigel-coated membrane (BD Bioscience, CA, USA) for invasion assay. As a chemoattractant, the bottom chamber was filled with complete medium supplemented with 10% FBS. After 48 h incubation, cells which did not invade through the membrane were swept with a cotton swab. Cells were then fixed with 20% methanol and stained with 0.2% crystal violet. Cells invaded into the bottom chamber per field were counted under inverted microscope (Olympus IX71, Tokyo, Japan).

Bioinformatics and Luciferase assay. miR-30a-5p target gene was predicted by Targetscan Release 7.2, the complementary sequences of FOXG1 and miR-30a-5p are shown in Figure 4A. For luciferase assay, SCL-1 cells were separated into blank and miR-30a-5p mimic groups and seeded in a 24-well plate at density of 5×10^4 cells/well. Quick-Change Site-Directed Mutagenesis kit (Stratagene, CA, USA) was used for the creation of the point mutation of FOXG1. Briefly, double-stranded oligonucleotides of wild or mutant type of FOXG1 were subcloned into the pGL3 Luciferase Reporter Vectors (E1751, Promega, WI, USA) by Shanghai Genepharma Company. Cells in miR-30a-5p mimic groups were co-transfected with miR-30a-5p and control vectors pRL-TK (Promega, WI, USA) while cells in blank group were transfected with control vectors alone. Transfection was performed by Lipofectamine™ 2000 (Invitrogen, Carlsbad, CA, USA). 24 h later, luciferase assays were performed by Dual-Glo luciferase assay kit (Promega, WI, USA). Luciferase activity was normalized to Renilla.

Quantitative PCR (qPCR). The total RNAs of SCL-1 and A431 cells were acquired using Trizol (Invitrogen, Waltham, USA). The generation of cDNA was from 1 µg isolated miRNA/mRNA using iScriptTMcDNA Synthesis Kit

(Bio-Rad, California, USA). For qPCR processing, Fast Start Universal SYBR Green Master kit (Roche, Basel, Switzerland) was used. The reaction system was prepared as follow: cDNA template 2.5 µl, forward primer (10 µM) 1 µl, reverse primer (10 µM) 1 µl, 2x SYBR Green master mix 10 µl, ddH_2O 5.5 µl. qPCR was performed following the procedures below: 2 min at 95 °C, 40 cycles of 15 sec at 95 °C, 25 sec at 60 °C and 60 sec at 72 °C. mRNA levels were normalized to GAPDH by $2^{-\Delta\Delta CT}$ method. Primers are exhibited in Table 1.

Western blot. Cells were harvested with ice-cold PBS and the whole cell proteins were extracted by ice-cold RIPA buffer mixed with protease inhibitors (ab65621, Abcam, San Francisco, USA). Protein lysate was separated by SDS-PAGE at 110 V for 100 min and transferred to PVDF membranes at 90 V for 90 min. PVDF membrane was blocked in 5% non-fat milk for 1 h at room temperature, and probed with anti-cleaved-Caspase 3 antibody (#9661, CST, MA, USA, 17 kDa), Bax (ab53154, Abcam, San Francisco, USA, 21 kDa), Bcl-2 (ab59348, Abcam, San Francisco, USA, 26 kDa) and anti-GAPDH antibody (ab8245, Abcam, San Francisco, USA, 36 kDa) at 1: 1000 dilution at 4 °C overnight. The membrane was further incubated with the second antibody IgG H&L (HRP) (ab6721, Abcam, San Francisco, USA, 1:2000) after the washing of membrane by PBST (PBS with 0.2% Tween 20). Protein blots band was detected by Pierce™ ECL plus western blotting substrate (Thermo Fisher, Waltham, USA) in ChemiDoc MP (Bio-Rad, California, USA). Grayscale of bolts were quantified by ImageJ software. The volume of each sample loaded in SDS-PAGE was normalized to the grayscale of GAPDH tested in the pilot study of western blot.

Statistical analysis. Data presented in this study were analyzed and visualized in GraphPad Prism Software Version 7.0. Student's t test and one-way analysis of variance (ANOVA) were used for the comparison. A p-value <0.05 indicated significant difference among groups.

Results

The elevation of miR-30a-5p expression suppressed the proliferation of SCL-1 and A431 cells. To figure out whether the expression of miR-30a-5p could affect the proliferation of cSCC cells, we explored the expression of miR-30a-5p in HaCaT, SCL-1 and A431 cells, and further investigated the alterations of EdU positive cells, colony number as well as cell cycle in SCL-1 and A431 cells, which carried an increased miR-30a-5p expression. As presented in the results, we observed that the expressions of miR-30a-5p in SCL-1 and A431 cells were significantly lower than in HaCaT cell (Figure 1A, **p<0.01, *p<0.05). When miR-30a-5p expression was elevated in SCL-1 and A431 cells successfully (Figure 1B, **p<0.01, ^^p<0.01), it showed significance that the EdU positive cells and colony number in miR-30a-5p mimic group was much lower than in blank and miControl group in both SCL-1 and A431 cells (Figures 1C, D, **p<0.01, *p<0.05, ^^p<0.01, ^p<0.05). Furthermore, the results of cell cycle assessment showed that the G1 phase in miR-30a-5p mimic group was significantly higher than in blank and miControl groups, while the S and G2 phases were much decreased in miR-30a-5p mimic group compared to blank and miControl groups in both SCL-1 and A431 cells (Figure 1E, **p<0.01, ^^p<0.01). Thus, it suggested that miR-30a-5p could be a regulator modulating the proliferation of SCL-1 and A431 cells.

The elevation of miR-30a-5p expression suppressed the migration and invasion rates of SCL-1 and A431 cells. Further, we investigated whether the migration and invasion rates of SCL-1 and A431 cells could be affected due to the upregulation of miR-30a-5p. As expected, we discovered that the migration and invasion rates in miR-30a-5p mimic groups were significantly lower than in blank and miControl groups in both SCL-1 and A431 cells (Figures 2A, B, **p<0.01, ^^p<0.01). It indicated that miR-30a-5p could also be a regulator modulating the capacity of metastasis of SCL-1 and A431 cells.

The elevation of miR-30a-5p expression regulated the expression of apoptosis related factors of SCL-1 and A431 cells. Furthermore, we investigated whether apoptosis related factors of SCL-1 and A431 cells could be affected due to the upregulation of miR-30a-5p as well. Here, we revealed that the mRNA and protein levels of Bcl-2 in miR-30a-5p mimic groups were decreased comparing to blank and miControl groups in SCL-1 and A431 cells, whereas the mRNA and protein levels of Bcl-2-associated X protein (Bax) and protein levels of cleaved Caspase-3 in miR-30a-5p mimic groups were dramatically higher than in blank and miControl groups in both SCL-1 and A431 cells (Figures 3A–C, **p<0.01, ^^p<0.01). It implied that the upregulation of miR-30a-5p could regulate the expression of apoptosis related factors of SCL-1 and A431 cells.

miR-30a-5p targeted FOXG1. To further clarify which gene that miR-30a-5p worked through, we identified whether FOXG1, the gene we predicted by bioinformatics, was the target of miR-30a-5p using luciferase assay, as well as measured the expressions of FOXG1 in SCL-1 and A431 cells in which the miR-30a-5p was elevated. The target sequence of miR-30a-5p on the 3'-UTR of FOXG1 is shown in Figure 4A. As presented in our results, the luciferase activity was decreased in miR-30a-5p mimic group compared to blank group when FOXG1 sequence was wild type whereas there was no significance between blank and miR-30a-5p mimic group when FOXG1 sequence was mutant (Figure 4B, **p<0.01, ^^p<0.01). Moreover, the relative mRNA and protein levels of FOXG1 in miR-30a-5p mimic groups were lower than in blank and miControl groups in both SCL-1 and A431 cells (Figures 4C, D, **p<0.01, ^^p<0.01). Taken together, it suggested that FOXG1 was the target of miR-30a-5p.

The upregulation of FOXG1 partially offsets the decreased proliferation due to the elevation of miR-30a-5p expression in SCL-1 and A431 cells. To affirm that FOXG1 could be the target of miR-30a-5p and therefore regulate the

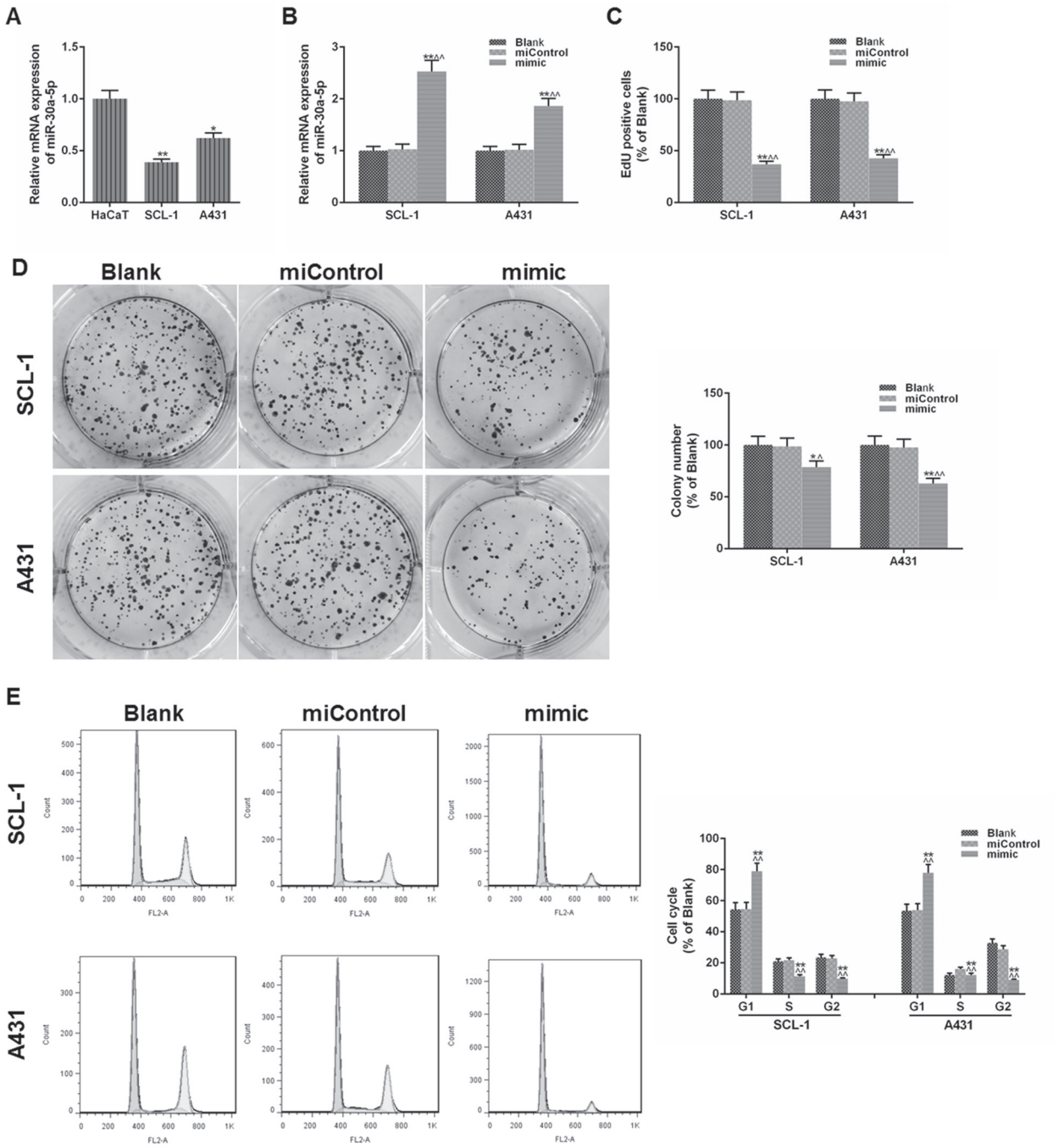

Figure 1. The effect of miR-30a-5p upregulation on the proliferation of SCL-1 and A431 cells in blank, miControl and miR-30a-5p mimic groups. A) The miR-30a-5p expressions in HaCaT, SCL-1 and A431 cells. B) The relative mRNA expression of miR-30a-5p in each group of SCL-1 and A431 cells. C) The 5-Ethynyl-2'-deoxyuridine (EdU) positive cells (% of blank) after 72 h in each group of SCL-1 and A431 cells. D) The colony number (% of blank) in each group of SCL-1 and A431 cells after 10 days. E) The G1, S and G2 phases (% of blank) in the cell cycle tested by flow cytometry in each group of SCL-1 and A431 cells after 24 h. Bars indicated means ± (standard deviation) SD. **p<0.01 and *p<0.05 vs. HaCaT cells or blank group; ^^p<0.01 and ^p<0.05 vs. miControl group.

proliferation of SCL-1 and A431 cells, we measured the alteration of colony numbers of SCL-1 and A431 cells in which the FOXG1 was upregulated. The mRNA and protein levels of FOXG1 were upregulated in cells transfected with FOXG1 (Figures 5A, B, **p<0.01, ##p<0.01). Here, we discovered that the colony numbers in FOXG1 and miR-30a-5p mimic + NC groups were higher and lower than in NC groups, respectively while they were lower and higher in miR-30a-5p mimic

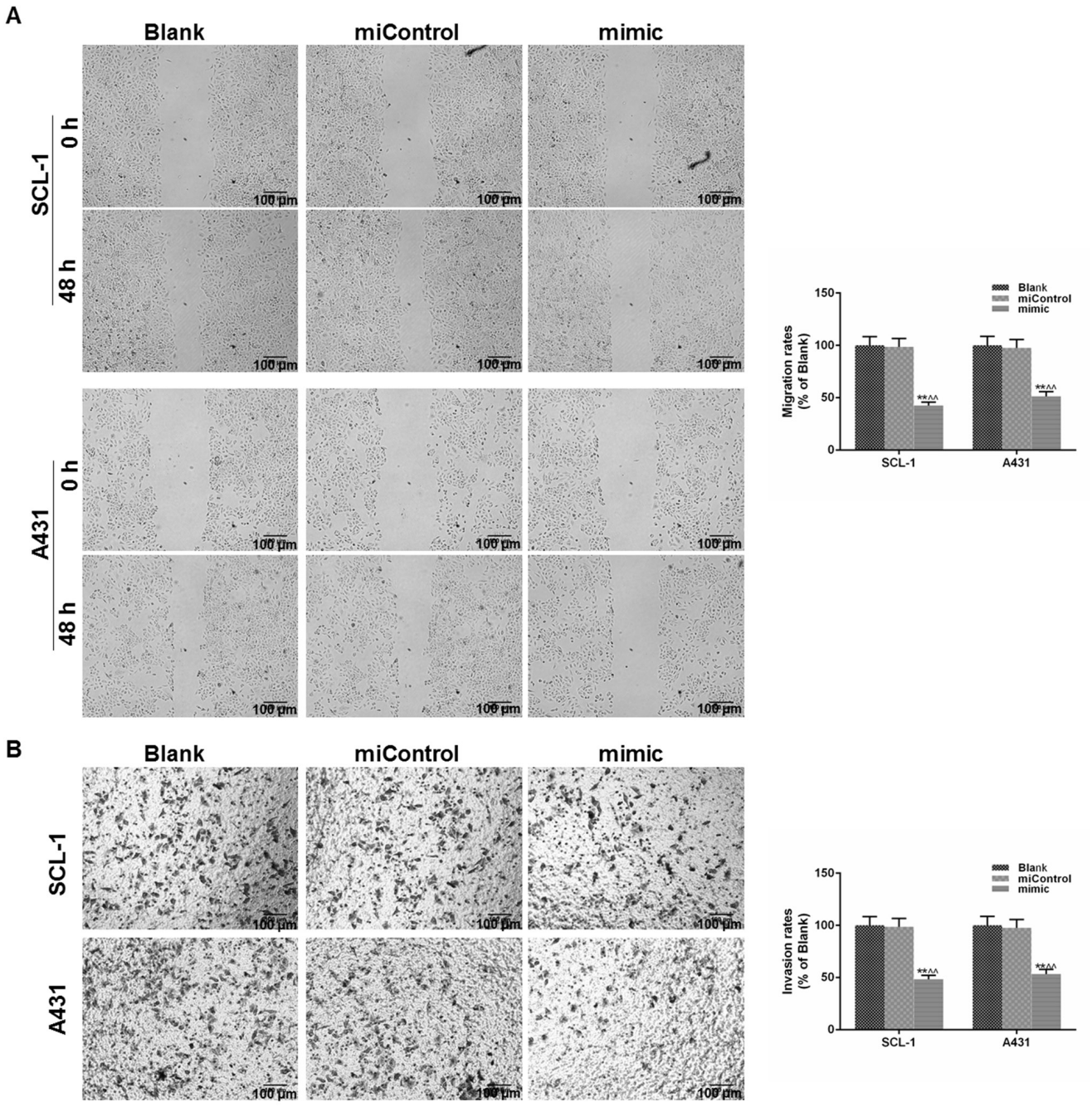

Figure 2. The effect of miR-30a-5p upregulation on the migration and invasion rates of SCL-1 and A431 cells in blank, miControl and miR-30a-5p mimic groups. A) The representative outcomes of wound healing assay after 48 h (×100 magnification) and the migration rates (% blank) in each group of SCL-1 and A431 cells. B) The representative outcomes of Transwell invasion assay after 48 h (×100 magnification) and the invasion rates (% blank) in each group of SCL-1 and A431 cells. Bars indicated means ± SD. **p<0.01 vs. blank group; ^^p<0.01 vs. miControl group.

+ FOXG1 group than in FOXG1 and miR-30a-5p mimic + NC groups, separately in both SCL-1 and A431 cells in which the FOXG1 expressions were upregulated (Figures 5C, D, $^{**}p<0.01$, $^{*}p<0.05$, $^{\wedge\wedge}p<0.01$, $^{\wedge}p<0.05$, $^{\#\#}p<0.01$, $^{\#}p<0.05$, $^{\&\&}p<0.01$, $^{\&}p<0.05$). It indicated that the upregulation of miR-30a-5p could target and downregulate FOXG1 expression and further decrease the proliferation of SCL-1 and A431 cells.

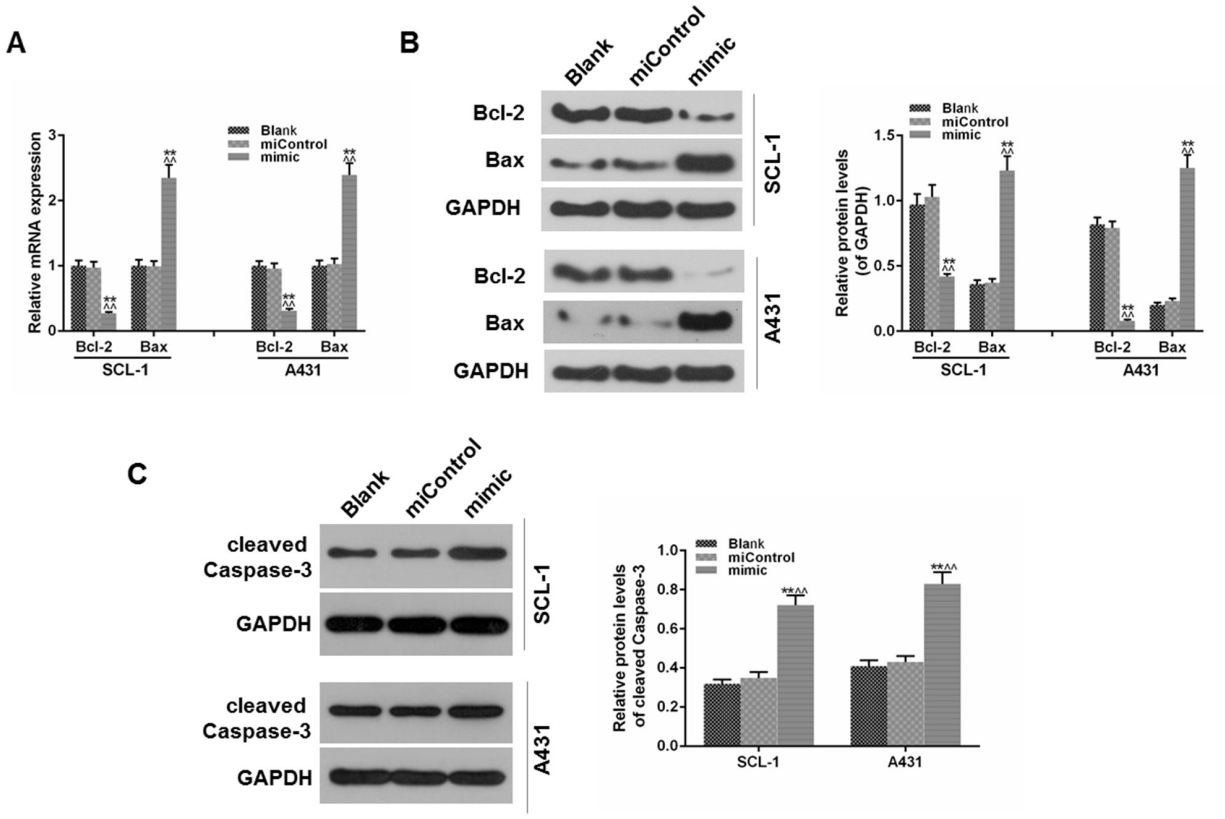

Figure 3. The effect of miR-30a-5p upregulation on the apoptosis of SCL-1 and A431 cells in blank, miControl and miR-30a-5p mimic groups. A) The relative mRNA expressions of Bcl-2 and Bax in each group of SCL-1 and A431 cells. B) The relative protein levels of Bcl-2 and Bax in each group of SCL-1 and A431 cells. C) The relative protein levels of cleaved Caspase-3 in each group of SCL-1 and A431 cells Bars indicated means ± SD. **p<0.01 vs. blank group; ^^p<0.01 vs. miControl group.

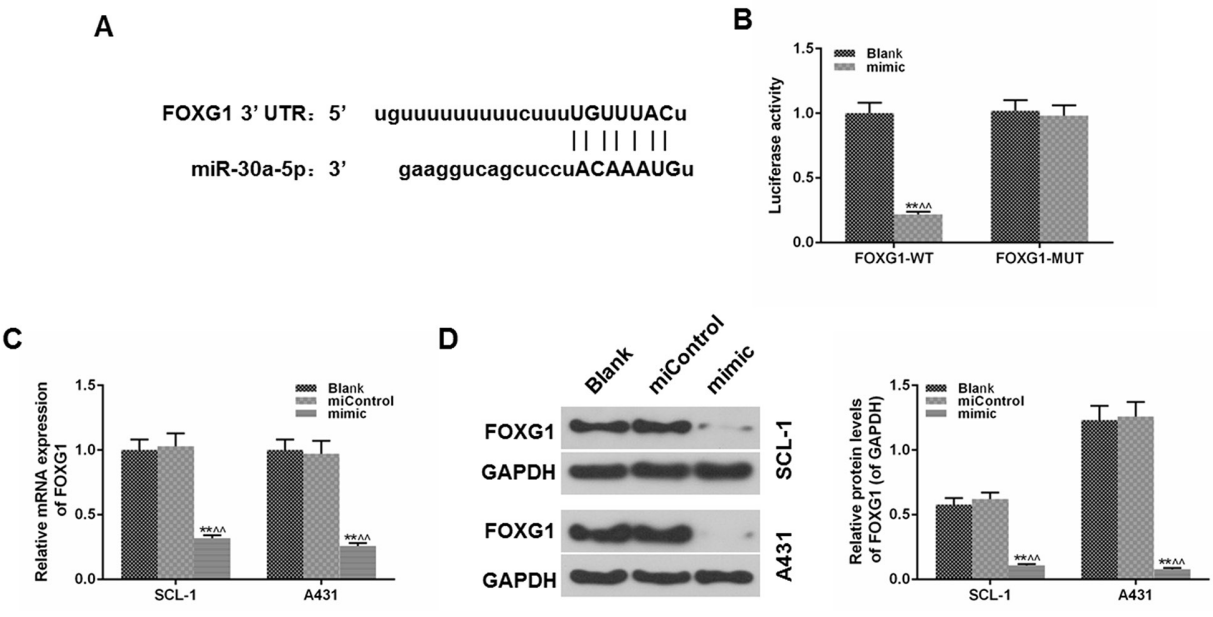

Figure 4. The identification of the target of miR-30a-5p. A) The possible complementary sequences of miR-30a-5p and forkhead box protein G1 (FOXG1) 3'-untranslated region (UTR). B) The luciferase activity in blank and miR-30a-5p mimic groups when the sequence of FOXG1 was wild type or mutant. C) The relative mRNA expression of FOXG1 in blank, miControl and miR-30a-5p mimic groups of SCL-1 and A431 cells. D) The protein levels of FOXG1 in blank, miControl and miR-30a-5p mimic groups of SCL-1 and A431 cells. Bars indicated means ± SD. **p<0.01 vs. blank group; ^^p<0.01 vs. miControl group.

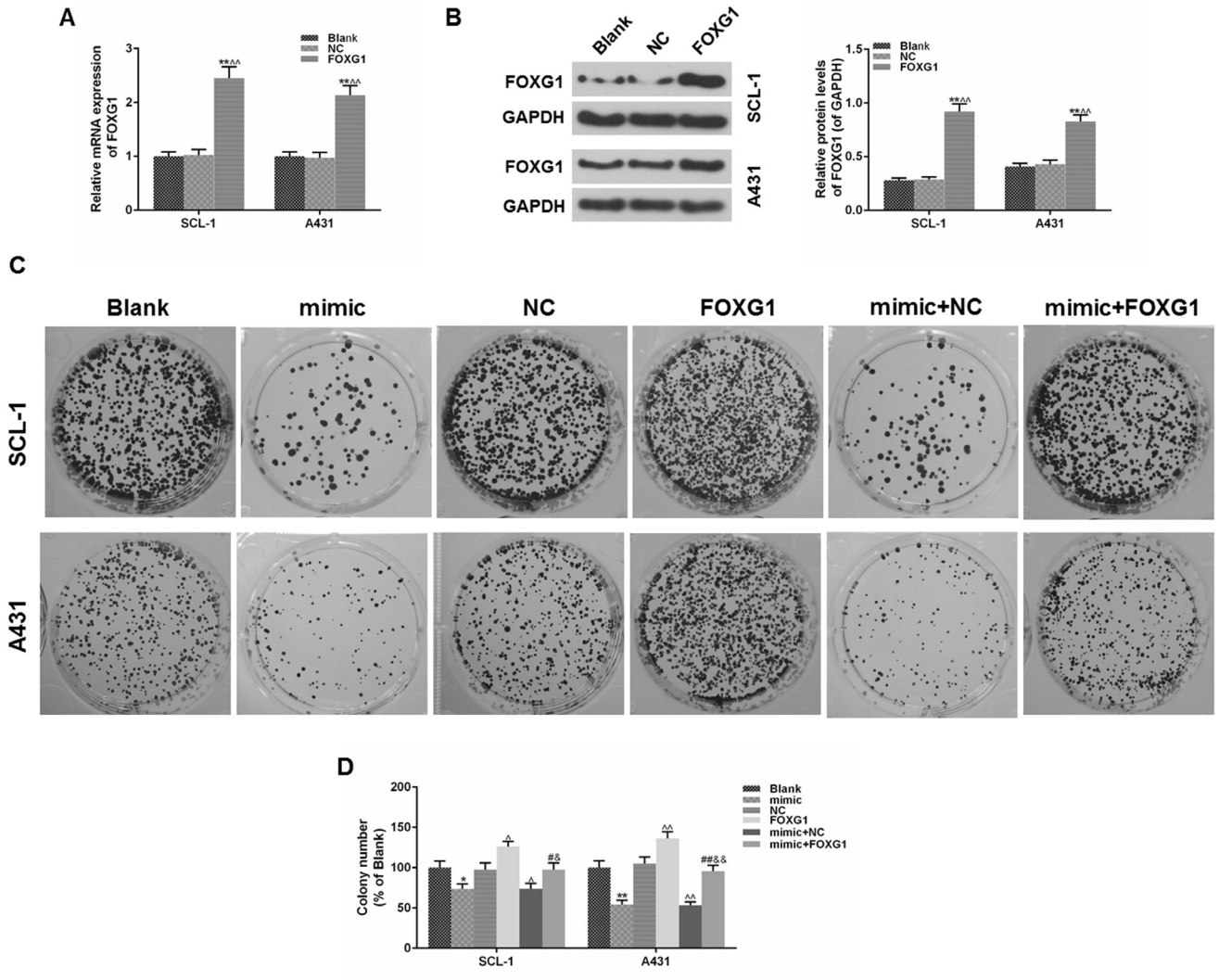

Figure 5. The confirmation of FOXG1 role of in the regulatory effect of miR-30a-5p on the SCL-1 and A431 cell proliferation. A) The relative mRNA expression of FOXG1 in blank, negative control (NC) and FOXG1 groups of SCL-1 and A431 cells. B) The relative protein levels of FOXG1 in blank, negative control (NC) and FOXG1 groups of SCL-1 and A431 cells. C and D) The colony numbers (% of blank) in blank, miR-30a-5p mimic, NC, FOXG1, miR-30a-5p mimic + NC and miR-30a-5p mimic + FOXG1 groups of SCL-1 and A431 cells after 48 h. Bars indicated means ± SD. **p<0.01 and *p<0.05 vs. blank group; ^^p<0.01 and ^p<0.05 vs. NC group; ##p<0.01 and #p<0.05 vs. FOXG1 group; &&p<0.01 and &p<0.05 vs. miR-30a-5p mimic + NC group.

The upregulation of FOXG1 partially offsets the decreased migration and invasion rates due to the elevation of miR-30a-5p expression in SCL-1 and A431 cells. To confirm that FOXG1 could be the target of miR-30a-5p and further regulate the migration and invasion rates of SCL-1 and A431 cells, we measured the alteration of migration and invasion rates of SCL-1 and A431 cells in which the FOXG1 were upregulated. Here, as the results showed, the migration and invasion rates in FOXG1 and miR-30a-5p mimic + NC groups were higher and lower than in NC groups, respectively while they were lower and higher in miR-30a-5p mimic + FOXG1 group than in FOXG1 and miR-30a-5p mimic + NC groups separately in both SCL-1 and A431 cells in which the FOXG1 expressions were upregulated (Figures 6A, B, C, D, **p<0.01, ^^p<0.01, ^p<0.05, #p<0.05, &&p<0.01). It suggested that the upregulation of miR-30a-5p could target and downregulate FOXG1 expression and further decrease the migration and invasion rates of SCL-1 and A431 cells.

Discussion

In this study, we found out that miR-30a-5p expression was decreased in SCL-1 and A431 cell lines, and its upregulation could suppress the proliferation, migration and invasion as well as raise the apoptosis of SCL-1 and A431 cells. Further, we also discovered that FOXG1 was the target of miR-30a-5p,

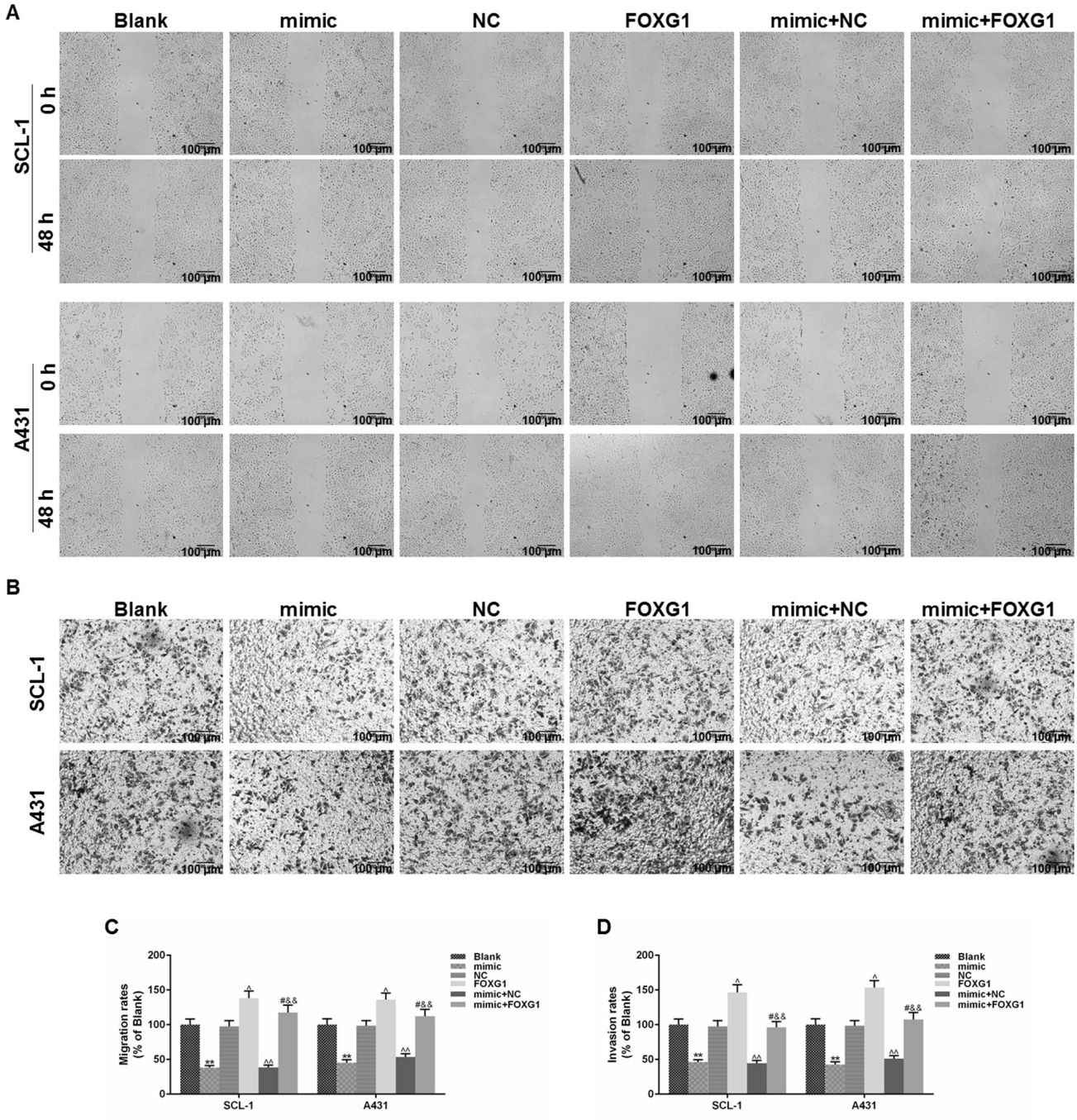

Figure 6. The confirmation of FOXG1 role of in the regulatory effect of miR-30a-5p on migration and invasion rates in blank, miR-30a-5p mimic, NC, FOXG1, miR-30a-5p mimic + NC, miR-30a-5p mimic + FOXG1 groups of SCL-1 and A431 cells. A) The representative outcomes of wound healing assay after 48 h in each group of SCL-1 and A431 cells (×100 magnification). B) The representative outcomes of Transwell invasion assay after 48 h in each group of SCL-1 and A431 cells (×100 magnification). C) The migration rates (% blank) in each group of SCL-1 and A431 cells. D) The invasion rates (% blank) in each group of SCL-1 and A431 cells. Bars indicated means ± SD. **p<0.01 vs. blank group; ^^p<0.01 and ^p<0.05 vs. NC group; #p<0.05 vs. FOXG1 group; &&p<0.01 vs. miR-30a-5p mimic + NC group.

which could be decreased by the upregulation of miR-30a-5p and therefore suppress the proliferation, migration and invasion of SCL-1 and A431 cells. Our study provided a novel pathway to interfere the development of cSCC.

Here, we observed that miR-30a-5p was downregulated in SCL-1 and A431 cells. miR-30a-5p expression was depressed in oral cavity cancer cells and was decreased in patients with cSCC as well [18, 19]. Our results are in accordance with the

outcomes previously reported, indicating that miR-30a-5p was surely downregulated in cSCC cells.

For the identification of miR-30a-5p role in regulation of critical cancer properties, we elevated the expression of miR-30a-5p in SCL-1 and A431 cells and further found out that the proliferation was decreased, the cell growth was suppressed, the cell cycle was arrested in G1 phase as well as the invasion and migration rates were depressed. Moreover, under the stimulation of apoptotic signals, Bcl-2 and Bax were activated and therefore transferred to the outer membrane of mitochondria, which elicited the release of cytochrome c and the activation of caspase-3, promoting apoptosis pathway [20, 21]. Thus, the decreased level Bcl-2 and increased levels of Bax and cleaved Caspase-3 proved that the expression of apoptosis related factors was regulated in the SCL-1 and A431 cell lines. As a limitation of the research, apoptosis rates influenced by miR-30a-5p overexpression was not studied. miR-30a-5p decreased cell growth and raised apoptosis rate of hepatocellular carcinoma cells [22]. miR-30a-5p overexpression inhibited cell proliferation, cell migration and invasion in non-small cell lung cancer cell lines [23]. Furthermore, the high expression of miR-30a-5p blocked chondrocytes in G0/G1 phase, reflecting that the highly expressed miR-30a-5p could affect the cell cycle to some extent [24]. In view of these findings, we speculated that the downregulated miR-30a-5p could be one cause promoting the development of cSCC.

For the exploration of the mechanism by which miR-30a-5p affects the cSCC properties, we identified that FOXG1 was the target of miR-30a-5p. Further, we discovered that the number of colony formations, migration and invasion rates were elevated in SCL-1 and A431 cells, which overexpressed miR-30a-5p and FOXG1 compared to cells that overexpressed miR-30a-5p only. FoxG1 is seen as a transcriptional repressor by binding to specific DNA sequences, belonging to Forkhead box family of transcription factors [25, 26]. Further, FoxG1 is a negative regulator of TGF-β signaling pathway, which is the basic of its oncogenic potential [27, 28]. Bulstrode et al. revealed that FOXG1 could control cell cycle in glioblastoma, enforcing the identity of neural stem cell [29]. He et al. demonstrated that that loss of FOXG1 promoted the growth of hair cells (HCs) and subsequent apoptosis of these HCs in mice [30]. Moreover, Ji et al. showed that the proliferation of non-small cell lung cancer was lifted by miR-378 via inhibiting FOXG1 [31]. In addition, Wu et al. exhibited that the invasion and metastasis was promoted by FOXG1 overexpression in colorectal cancer cells [32]. Unfortunately, no report had declared the role of FOXG1 in cSCC, according to our investigation. Thus, taken these findings together, we speculated that the decreased expression of FOXG1 caused by the downregulated miR-30a-5p could be one possible mechanism leading to the development of cSCC.

In summary, miR-30a-5p acted as a regulatory role on the expression of FOXG1 and further modulated the progressing of cSCC cells, which could be a novel pathway intervening the development of cSCC.

References

[1] TUFARO AP, CHUANG JC, PRASAD N, CHUANG A, CHUANG TC et al. Molecular markers in cutaneous squamous cell carcinoma. Int J Surg Oncol 2011; 2011: 231475. https://doi.org/10.1155/2011/231475

[2] YESANTHARAO P, WANG W, IOANNIDIS NM, DEMEHRI S, WHITTEMORE AS et al. Cutaneous squamous cell cancer (cSCC) risk and the human leukocyte antigen (HLA) system. Hum Immunol 2017; 78: 327–335. https://doi.org/10.1016/j.humimm.2017.02.002

[3] BURTON KA, ASHACK KA, KHACHEMOUNE A. Cutaneous Squamous Cell Carcinoma: A Review of High-Risk and Metastatic Disease. Am J Clin Dermatol 2016; 17: 491–508. https://doi.org/10.1007/s40257-016-0207-3

[4] UNSAL AA, UNSAL AB, HENN TE, BAREDES S, ELOY JA. Cutaneous squamous cell carcinoma of the lip: A population-based analysis. Laryngoscope 2018; 128: 84–90. https://doi.org/10.1002/lary.26704

[5] WEISTENHOFER W, HILLER J, DREXLER H, KIESEL J. Retrospective evaluation of exposure to natural UV radiation: experiences with the online UV history tool in a field study. J Dtsch Dermatol Ges 2017; 15: 610–619. https://doi.org/10.1111/ddg.13250

[6] ZAMOISKI RD, YANIK E, GIBSON TM, CAHOON EK, MADELEINE MM et al. Risk of Second Malignancies in Solid Organ Transplant Recipients Who Develop Keratinocyte Cancers. Cancer Res 2017; 77: 4196–4203. https://doi.org/10.1158/0008-5472.CAN-16-3291

[7] SATGUNASEELAN L, CHIA N, SUH H, VIRK S, ASHFORD B et al. p16 expression in cutaneous squamous cell carcinoma of the head and neck is not associated with integration of high risk HPV DNA or prognosis. Pathology 2017; 49: 494–498. https://doi.org/10.1016/j.pathol.2017.04.002

[8] YEN H, DHANA A, OKHOVAT JP, QURESHI A, KEUM N et al. Alcohol intake and risk of nonmelanoma skin cancer: a systematic review and dose-response meta-analysis. Br J Dermatol 2017; 177: 696–707. https://doi.org/10.1111/bjd.15647

[9] PATEL TN, PATEL SB, FRANCA K, CHACON AH, NOURI K. Mohs micrographic surgery: history, technique, and advancements. Skinmed 2014; 12: 289–292.

[10] KESTY K, SANGUEZA OP, LESHIN B, ALBERTINI JG. Mohs micrographic surgery and dermatopathology concordance; An analysis of 1421 Mohs cases over 17 years. J Am Acad Dermatol 2017. https://doi.org/10.1016/j.jaad.2017.11.055

[11] MANSOURI B, BICKNELL LM, HILL D, WALKER GD, FIALA K et al. Mohs Micrographic Surgery for the Management of Cutaneous Malignancies. Facial Plast Surg Clin North Am 2017; 25: 291–301. https://doi.org/10.1016/j.fsc.2017.03.00

[12] ACUNZO M, ROMANO G, WERNICKE D, CROCE CM. MicroRNA and cancer – a brief overview. Adv Biol Regul 2015; 57: 1–9. https://doi.org/10.1016/j.jbior.2014.09.013

[13] MOHR AM, MOTT JL. Overview of microRNA biology. Semin Liver Dis 2015; 35: 3–11. https://doi.org/10.1055/s-0034-1397344

[14] ACUNZO M, CROCE CM. MicroRNA in Cancer and Cachexia--A Mini-Review. J Infect Dis 2015; 212 Suppl 1: S74–77. https://doi.org/10.1093/infdis/jiv197

[15] QI B, WANG Y, CHEN ZJ, LI XN, QI Y et al. Down-regulation of miR-30a-3p/5p promotes esophageal squamous cell carcinoma cell proliferation by activating the Wnt signaling pathway. World J Gastroenterol 2017; 23: 7965–7977. https://doi.org/10.3748/wjg.v23.i45.7965

[16] WANG Y, WU C, ZHANG C, LI Z, ZHU T et al. TGF-beta-induced STAT3 overexpression promotes human head and neck squamous cell carcinoma invasion and metastasis through malat1/miR-30a interactions. Cancer Lett 2018; 436: 52–62. https://doi.org/10.1016/j.canlet.2018.08.009

[17] TANG R, LIANG L, LUO D, FENG Z, HUANG Q et al. Downregulation of MiR-30a is Associated with Poor Prognosis in Lung Cancer. Med Sci Monit 2015; 21: 2514–2520. https://doi.org/10.12659/MSM.894372

[18] RUAN P, TAO Z, TAN A. Low expression of miR-30a-5p induced the proliferation and invasion of oral cancer via promoting the expression of FAP. Biosci Rep 2018; 38. https://doi.org/10.1042/BSR20171027

[19] SAND M, SKRYGAN M, GEORGAS D, SAND D, HAHN SA et al. Microarray analysis of microRNA expression in cutaneous squamous cell carcinoma. J Dermatol Sci 2012; 68: 119–126. https://doi.org/10.1016/j.jdermsci.2012.09.004

[20] GREEN DR, LLAMBI F. Cell Death Signaling. Cold Spring Harb Perspect Biol 2015; 7. https://doi.org/10.1101/cshperspect.a006080

[21] HASSAN M, WATARI H, ABUALMAATY A, OHBA Y, SAKURAGI N. Apoptosis and molecular targeting therapy in cancer. Biomed Res Int 2014; 2014: 150845. https://doi.org/10.1155/2014/150845

[22] HE R, YANG L, LIN X, CHEN X, LIN X et al. MiR-30a-5p suppresses cell growth and enhances apoptosis of hepatocellular carcinoma cells via targeting AEG-1. Int J Clin Exp Pathol 2015; 8: 15632–15641.

[23] ZHU J, ZENG Y, LI W, QIN H, LEI Z et al. CD73/NT5E is a target of miR-30a-5p and plays an important role in the pathogenesis of non-small cell lung cancer. Mol Cancer 2017; 16: 34. https://doi.org/10.1186/s12943-017-0591-1

[24] SHEN PF, QU YX, WANG B, XU JD, WEI K et al. [miR-30a-5p promotes the apoptosis of chondrocytes in patients with osteoarthritis by targeting protein kinase B]. Zhonghua Yi Xue Za Zhi. 2017; 97: 3079–3084. https://doi.org/10.3760/cma.j.issn.0376-2491.2017.39.008

[25] OBENDORF M, MEYER R, HENNING K, MITEV YA, SCHRODER J et al: FoxG1, a member of the forkhead family, is a corepressor of the androgen receptor. J Steroid Biochem Mol Biol 2007; 104: 195–207. https://doi.org/10.1016/j.jsbmb.2007.03.012

[26] BOGGIO EM, PANCRAZI L, GENNARO M, LO RIZZO C, MARI F et al. Visual impairment in FOXG1-mutated individuals and mice. Neuroscience 2016; 324: 496–508. https://doi.org/10.1016/j.neuroscience.2016.03.027

[27] CHAN DW, LIU VW, TO RM, CHIU PM, LEE WY et al. Overexpression of FOXG1 contributes to TGF-beta resistance through inhibition of p21WAF1/CIP1 expression in ovarian cancer. Br J Cancer 2009; 101: 1433–1443. https://doi.org/10.1038/sj.bjc.6605316

[28] ZENG F, XUE M, XIAO T, LI Y, XIAO S et al. MiR-200b promotes the cell proliferation and metastasis of cervical cancer by inhibiting FOXG1. Biomed Pharmacother 2016; 79: 294–301. https://doi.org/10.1016/j.biopha.2016.02.033

[29] BULSTRODE H, JOHNSTONE E, MARQUES-TORREJON MA, FERGUSON KM, BRESSAN RB et al. Elevated FOXG1 and SOX2 in glioblastoma enforces neural stem cell identity through transcriptional control of cell cycle and epigenetic regulators. Genes Dev 2017; 31: 757–773. https://doi.org/10.1101/gad.293027.116

[30] HE Z, FANG Q, LI H, SHAO B, ZHANG Y et al. The role of FOXG1 in the postnatal development and survival of mouse cochlear hair cells. Neuropharmacology 2018; 144: 43–57. https://doi.org/10.1016/j.neuropharm.2018.10.021

[31] JI KX, CUI F, QU D, SUN RY, SUN P et al. MiR-378 promotes the cell proliferation of non-small cell lung cancer by inhibiting FOXG1. Eur Rev Med Pharmacol Sci 2018; 22: 1011–1019. https://doi.org/10.26355/eurrev_201802_14383

[32] WU H, QIAN C, LIU C, XIANG J, YE D et al. [Role and mechanism of FOXG1 in invasion and metastasis of colorectal cancer]. Sheng Wu Gong Cheng Xue Bao 2018; 34: 752–760. https://doi.org/10.13345/j.cjb.170389